JOURNAL OF APPLIED ELECTROCHEMISTRY **28** (1998) 1343–1349

# Theoretical limiting prediction of $H_2S$ removal efficiency from coal gasification streams using an intermediate temperature electrochemical separation process

J. S. ROBINSON, J. WINNICK

*School of Chemical Engineering, Georgia Institute of Technology, Atlanta, GA 30332, USA*

Received 27 January 1997; accepted in revised form 8 September 1997

A mathematical model has been developed to predict the theoretical limiting $H_2S$ removal efficiency of an electrochemical membrane separator (EMS) in the presence of overwhelming levels of $H_2O$ and $CO_2$ (as would be found in syn-gas). Thermodynamic principles gave the minimum potential requirements for cell operation. Factors including electrokinetics, mass transfer, chemical equilibria and internal resistance, occuring with application of current, were incorporated into the prediction. Theoretical predictions, which represent a limiting value, show achievable current efficiencies close to 100% for high $H_2S$ levels (1000 ppm) at 90% removal. At this same removal level with 100 or 10 ppm inlet gas, the predicted maximum current efficiencies dropped, due to concentration effects, to 93% and 40%, respectively. This solidifies the economic importance of obtaining close to 100% current efficiencies at sour gas levels compared to polishing applications where the removal, not the current efficiency, is more important. Predicted cell potentials were consistently in the same range, $-0.450$ to $-0.550$ V, for all concentration levels at 90% removal. Comparison with experimental data gave good agreement; actual current efficiencies were consistently within 15% of the maximum predicted values at coinciding removal levels. However, actual potentials were lower (less negative) because of hydrogen leakage through the cell membrane. While lower potentials require less power, sulfur production at the anode was reduced.

Keywords: *coal gas*, *electrochemical separation*, *hydrogen sulfide*, *membrane*, *removal efficiency model*

## 1. Introduction

Processes to remove $H_2S$ typically rely on low-to-ambient temperature adsorption, followed by sorbent regeneration and Claus plant treatment for conversion of $H_2S$ to a salable byproduct, sulfur. Although effective, this type of removal is very process-intensive as well as energy-inefficient due to low temperature operation. Gasification streams generally range from 500–1000 °C, requiring cooling before and reheating after process gas sweetening. Although these technologies have proven capable of meeting $H_2S$ levels required by MCFC, there are several disadvantages inherent to these processes [1, 2].

Alternative high temperature methods are presently available, but process drawbacks including morphological changes in catalytic beds [3] or inefficient molten salt sorbent processes [4] that negate savings incurred through energy efficient removal temperatures.

An electrochemical membrane has been shown to remove $H_2S$ from coal gas streams in laboratory tests [5–7]. The high operating temperature, flow-through design, capability of selective $H_2S$ removal and direct production of elemental sulfur offered by this process provide several advantages over existing and developmental $H_2S$ removal technologies.

But, coal gasification streams contain a considerable concentration of electro-active species (i.e. $CO_2$, $H_2O$), up to five orders of magnitude greater than $H_2S$, creating a competition for the electrons at the cathode. However, the effect of the Nernst equation is to cause large concentration differences to be commensurate with only small differences in total cell potential.

The electrochemical membrane separator (EMS) [5–7], the focus of the limiting prediction studies, purges a fuel gas contaminated with $H_2S$. This is done by reducing the most electroactive species in the gas stream. In this case, $H_2S$ is reduced by the following:

$$H_2S + 2e^- \longrightarrow H_2 + S^{2-} \quad (1)$$

A membrane which contains sulfide ions in a molten salt electrolyte will act to transport the ions across to the anode. If the membrane is impermeable to $H_2$ diffusion from the cathode side, an inert sweep gas can be used to carry the vaporous oxidized sulfur downstream to be condensed:

$$S^{2-} \longrightarrow \tfrac{1}{2}S_2 + 2e^- \quad (2)$$

The situation is somewhat complicated when real gas mixtures are processed. Carbon dioxide and wa-

0021-891X  

ter vapor compete in the reduction reaction at the cathode by

$$CO_2 + H_2O + 2e^- \longrightarrow H_2 + CO_3^{2-} \quad (3)$$

The ionic flux through the membrane depends on both the relative mobilities of carbonate and sulfide ions as well as their concentrations.

However, anodic competition exists in the form of carbonate oxidation:

$$CO_3^{2-} \longrightarrow CO_2 + \tfrac{1}{2}O_2 + 2e^- \quad (4)$$

Preventing the oxidation of carbonate at the anode is necessary for prohibiting its transport through the membrane, allowing the preferred oxidation of sulfide ions, Reaction 2.

## 2. Background

Membrane gas separation systems have been used in applications, such as hydrogen gas purification, for many years. The separation relies on a chemical potential gradient as the driving force. A pressure or concentration gradient usually provides the necessary driving force for mass transfer of component $i$ across the membrane:

$$\Delta\mu_i = \mu_i - \mu_i' = RT \ln\left(\frac{a_i}{a_i'}\right) \quad (5)$$

where the prime represents the extractive side. Typically, these processes are not species selective; therefore, they do not produce high purity products.

In an electrochemical membrane separation, an electrochemical potential gradient provides the driving force across the membrane:

$$\Delta\overline{\mu} = \overline{\mu_i} - \overline{\mu_i'} = RT \ln\left(\frac{a_i}{a_i'}\right) + z_i F \Delta\Phi \quad (6)$$

which is established by applying an external potential, $\phi$. In this case, with charged species, a pressure or concentration gradient is neither required nor desired. However, to establish the validity of this device for application to coal gasification cleansing, it is necessary to quantify the maximum current efficiency achievable at various levels of $H_2S$ in the presence of competing species (e.g. $CO_2$ and $H_2O$).

## 3. Prediction of limiting performance

A high temperature electrochemical membrane process is illustrated in Fig. 1. Summing the commensurable half-cell reactions at 923 K, shown in Fig. 2 on a potential scale based on the carbonate reference used in molten carbonate research, from Equations 1 and 2 results in

$$H_2S \longrightarrow H_2 + \tfrac{1}{2}S_2 \quad E^\circ = -0.239\,\text{V} \quad (7)$$

and from Equations 3 and 4 yields

$$H_2O \longrightarrow H_2 + \tfrac{1}{2}O_2 \quad E^\circ = -1.030\,\text{V} \quad (8)$$

which can be related to the change in standard Gibb's energy and minimum electrical work required for the separation by

$$W_e = \Delta G = -nFE^\circ \quad (9)$$

where $n$ is the number of electrons transferred in the reaction and $F$ is Faraday's constant or the amount of charge passed per mole of species reduced or oxidized. Negative $E^\circ$ values indicate a nonspontaneous process; reactions with smaller negative values will be most likely to proceed. Thus, at low cell potentials sulfide ions will be transported in preference to carbonate. Each will occur at the *same cell potential*; that is, the total cell voltage less the ohmic polarization. But as expressed by the Nernst relation, the concen-

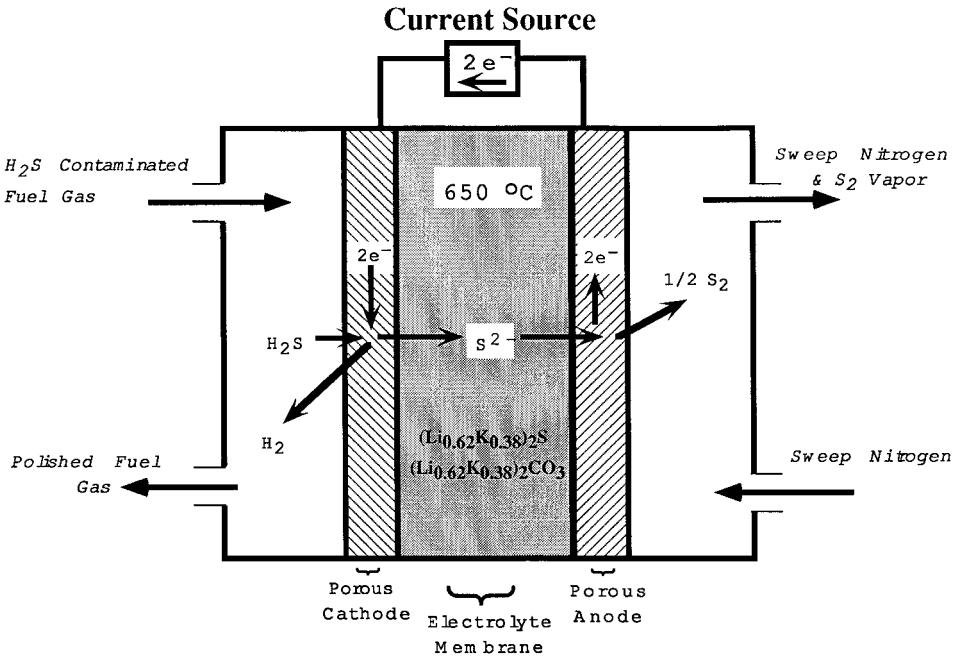


Fig. 1. Single-cell view of the electrochemical membrane separator.

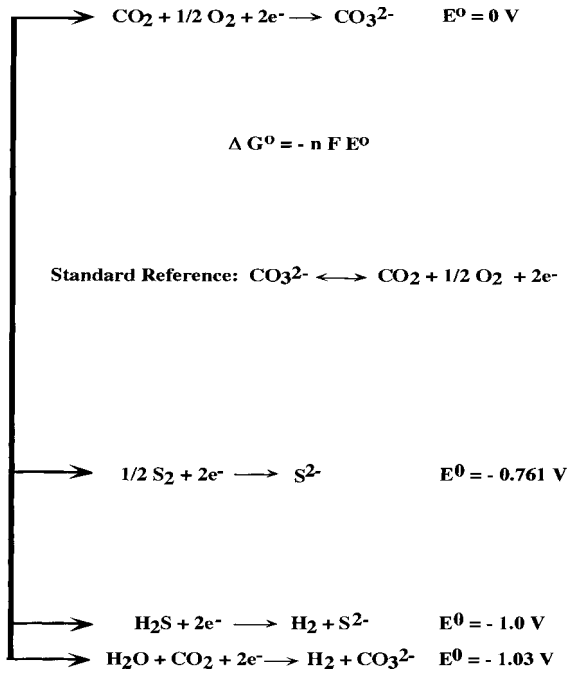


Fig. 2. Half-cell reactions on a potential scale (vs standard reference).

tration terms will be greatly affected by the large difference in the standard cell potential, $E^\circ$, values.

$$E = E_7^\circ - \left(\frac{RT}{nF}\right)\ln\left\{\frac{a_{S^{2-}_{cath}} P_{H_2\,cath} P^{1/2}_{S_2\,an}}{a_{S^{2-}_{an}} P_{H_2S_{cath}}}\right\} \quad (10)$$

$$E = E_8^\circ - \left(\frac{RT}{nF}\right)\ln\left\{\frac{a_{CO^{2-}_{3\,cath}} P_{H_2\,cath} P_{CO_2\,an} P^{1/2}_{O_2\,an}}{a_{CO^{2-}_{3\,an}} P_{CO_2\,cath} P_{H_2O\,cath}}\right\} \quad (11)$$

In addition to the Nernst potential, additional applied voltage is required to operate the separation cell due to irreversible losses. These losses occur by internal resistance, concentration effects in the process gases, and the activation barrier for electron transfer. The result is an increase in the total cell potential over the reversible potential.

### 3.1. *Activation overpotential*

The activation overpotential at both cathode and anode is the overpotential required to drive the electrochemical reactions occurring at these electrodes. The expression relating this overpotential to the flux, or current density, is the Butler–Volmer equation:

$$i = i_0\left[\exp\left(\frac{\alpha_a F \eta_{act,a}}{RT}\right) - \exp\left(\frac{-\alpha_c F \eta_{act,c}}{RT}\right)\right] \quad (12)$$

which holds for specified temperature, pressure, and concentration of reacting species. The transfer coefficients, $\alpha_a$ and $\alpha_c$, sum to the number of electrons transferred in the reaction:

$$\alpha_a + \alpha_c = n \quad (13)$$

### 3.2. *Concentration overpotential*

Concentration overpotential originates from developing concentration gradients due to consumption of electro-active species at the electrode surface. Transport of these species is composed of four steps, occurring in series: (i) the $H_2S$ must diffuse through the gas-phase boundary layer to the cathode interface, (ii) it must diffuse through the pores of the electrode to the electrolyte film, (iii) the sulfide ion must migrate to the anode, and (iv) the oxidized species must diffuse out into the sweep gas at the anode. The effect of step (iii) has been minimized due to proper membrane design and steps (ii) and (iv) have been found to be of no consequence [8–10]. The limiting process for removal is thus diffusion of electroactive species to the electrode pores from the bulk gas. Since the gas-phase concentration of $H_2S$ changes along the length of the channels, a log-mean average is used in the calculation of limiting current density by:

$$i_L = nFk_m\rho\frac{(y_{inlet} - y_{exit})}{\ln(y_{inlet}/y_{exit})} \quad (14)$$

where $n$ is the number of electrons transferred per mole of species removed, $F$ is Faraday's constant, $k_m$ is mass transfer coefficient, $\rho$ is the molar density of the bulk gas, and $y_x$ is the inlet or exit mole fraction of $H_2S$. The average mass transfer coefficient was derived from an estimated Sherwood number dependent on channel dimension and constant $H_2S$ surface concentration 11 as follows:

$$N_{Sh} = \frac{k_m D_{eq}}{D_{ab}} \quad (15)$$

with $D_{eq}$ defined as the equivalent channel diameter above the electrode surface:

$$D_{eq} = 4r_h = \frac{4(\text{cross-sectional area})}{(\text{wetted perimeter})} \quad (16)$$

For our square channel and laminar flow the Sherwood number is 2.98 [11]. The diffusion coefficient of $H_2S$ through nitrogen at 650 °C is calculated by [12]

$$D_{ab} = \frac{0.001\,858\,3\,T^{3/2}}{P\sigma_{ab}\Omega_{D_{ab}}}\sqrt{\frac{1}{M_a} + \frac{1}{M_b}} \quad (17)$$

In these experiments, $D_{eq}$ is 0.3 cm, $D_{ab}$ is 1.1 $cm^2\ s^{-1}$, giving a mass transfer coefficient of 11.2 $cm\ s^{-1}$.

The concentration overpotential is expressed in terms of applied current and the limiting current density found from Equation 14 by

$$\eta_{conc} = \frac{RT}{nF}\ln\left(1 - \frac{i}{i_l}\right) \quad (18)$$

For example, at 90% $H_2S$ removal from 1000 ppm inlet, at 200 $cm^3\ min^{-1}$, the calculated limiting and stoichiometric current densities are 118.1 $A\ m^{-2}$ and 29.6 $A\ m^{-2}$, respectively, with an electrode area of $7.91 \times 10^{-4}\ m^2$.

The stoichiometric current density required to remove a percentage of inlet $H_2S$ is given by

$$i = \frac{nFP\dot{V}}{RT}\left(\Delta x_{\text{species removed}}\right) \quad (19)$$

Dividing by the limiting current density gives the minimum electrode area necessary for these removals:

$$\text{Electrode area} = \frac{i}{i_L} \tag{20}$$

before exceeding the limiting current based on bulk-gas diffusion of $H_2S$.

### 3.3. *Ohmic polarization*

Ohmic losses occur due to resistance in ionic and electronic transfer of current through the separation system. The ohmic losses can be expressed by

$$E_{\text{ohmic}} = IR \tag{21}$$

with $I$ representing current and $R$ the total cell resistance.

### 3.4. *Cell voltage*

Total cell voltage incorporating *ohmic* polarization, *concentration* and *activation* overpotentials along with the Nernstian effects (Equation 10) sums to

$$V_{\text{cell}} = \Delta E_{\text{c-a}} - |\eta_{\text{conc}}| - |\eta_{\text{act}}| - IR \tag{22}$$

where $\Delta E_{\text{c-a}}$ is the equilibrium cell voltage. Although as we will see, the driving force for each of the electrode reactions is independent of the ohmic effects in the present case.

The relative contribution of each variable in the cell voltage can be graphed against the percentage $H_2S$ removal in an attempt to ascertain the most outstanding energy loss mechanism. Process improvements in these areas can reduce the energy input needed to obtain $H_2S$ removals.

## 4. Discussion of theoretical limiting prediction

The simulated run conditions were at equal cathodic and anodic flow rates of 200 $cm^3\,min^{-1}$, atmospheric system pressure, a run temperature of 650 °C, and three order of magnitude changes in $H_2S$ removal (1000 to 1 ppm). The superficial cathodic and anodic exchange current densities were estimated at 40 $mA\,cm^{-2}$ after the results of the free electrolyte studies [8, 9]. The exchange coefficients, $\alpha_a$ and $\alpha_c$, were assumed to be unity. Ohmic resistance across the cell was conservatively estimated to be 1 Ω, based on past EMS experiments [5–7].

The above exchange current densities were used in Equation 12 at the stoichiometric current densities corresponding to each flow rate of $H_2S$. As shown in Figs 3, 4 and 5, calculated activation overpotentials are negligible at both cathode and anode. This means the electrochemical kinetics are extremely rapid as compared with diffusion from the bulk gas phase and through the electrolyte filled membrane. Calculated cross-cell voltages are shown as the sum of the Nernstian, concentration, and ohmic polarization effects. Therefore, at 90% removal $H_2S$ (1000–100 ppm; 100–10 ppm; 10–1 ppm), the results of Figs. 3, 4 and 5 predict total cross-cell voltages of −0.4474, −0.4675 and −0.5107 V.

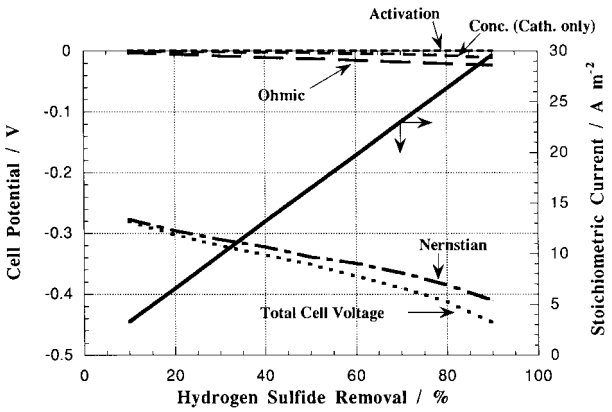


Fig. 3. Theoretical cross-cell potential against $H_2S$ removal. 1000 ppm inlet.

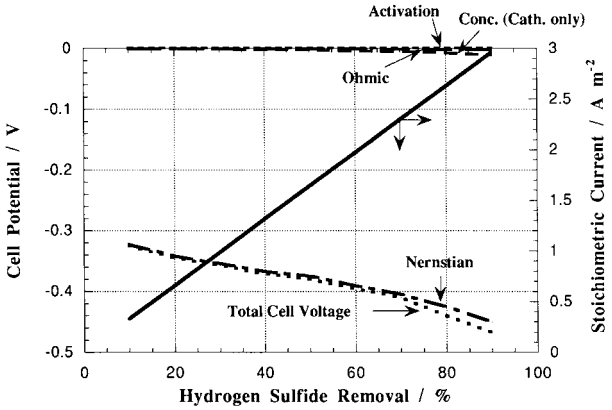


Fig. 4. Theoretical cross-cell potential against $H_2S$ removal. 100 ppm inlet.

### 4.1. *Parallel sulfide, carbonate transport*

Since the carbonate transport of Reaction 8 parallels the sulfide transport of Reaction 7, the same current is available for transport of both species. Therefore, only a certain amount of current will act to transport either constituent, giving a finite maximum current efficiency with respect to $H_2S$ removal for any percentage of $H_2S$ removed. This is dependent on gas composition and total cross-cell potential required for the desired separation of $H_2S$.

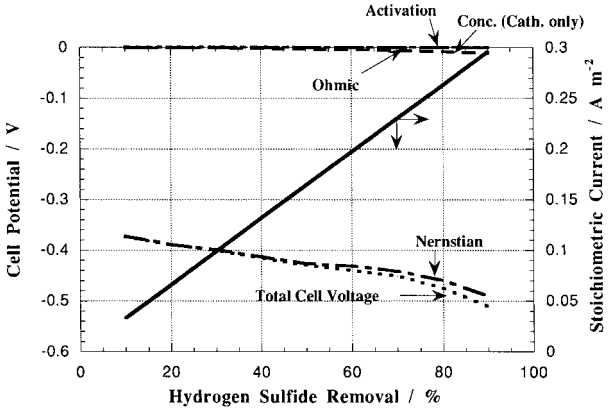


Fig. 5. Theoretical cross-cell potential against $H_2S$ removal. 10 ppm inlet.

The total cross-cell voltage is calculated for the desired $H_2S$ removal from Equation 22, assuming: equal cathode and anode gas flow rates, and that the equilibrium voltage calculated from the Nernst expression, Equation 10 and the $H_2S$ concentration overpotential, Equation 18 are the only significant contributions to the total cell voltage. Further, at the low fluxes encountered here, the activity of sulfide is assumed equal at cathode and anode.

The Nernst potential for carbonate (Equation 11) can be equated to this total cross-cell voltage, since both occur at the same potential. Note there is no contribution of concentration overpotential for carbon dioxide or water at the cathode, due to their high levels relative to $H_2S$, and there is negligible activation overpotential at these low current densities. From this potential, the $CO_2$ partial pressure at the anode is calculated (the $O_2$ partial pressure is one-half the $CO_2$ partial pressure). The calculated extent of parasitic carbonate current occurring in the removal cell as a function of percentage $H_2S$ removal is shown in Figs 6, 7 and 8 as anodic $CO_2$ partial pressure and current efficiency.

Examination of the results shows that the theoretical maximum $H_2S$ current efficiency drops only to 99.5% at 90% $H_2S$ removal (1000–100 ppm $H_2S$), 93.2% at 90% $H_2S$ removal (100–10 ppm $H_2S$), and 40.2% at 90% $H_2S$ removal (10–1 ppm $H_2S$). The excess current goes to produce anodic $CO_2$. Although attempts were made to measure $CO_2$ evolution, none was observed. This is no doubt due to the fact that it was below detectable levels. No $H_2S$ was ever detected at the anode.

### 4.2. *$H_2$ crossover*

Hydrogen crossover is another deterrent in obtaining higher current efficiencies; however, its effect was not incorporated into the theoretical model. When $H_2$ crossover from the cathode side to the anode side occurs, two reactions are possible at the anode. The first is the oxidation of hydrogen and the sulfide ion to hydrogen sulfide by

$$H_2 + S^{2-} \longrightarrow H_2S + 2e^- \qquad (23)$$

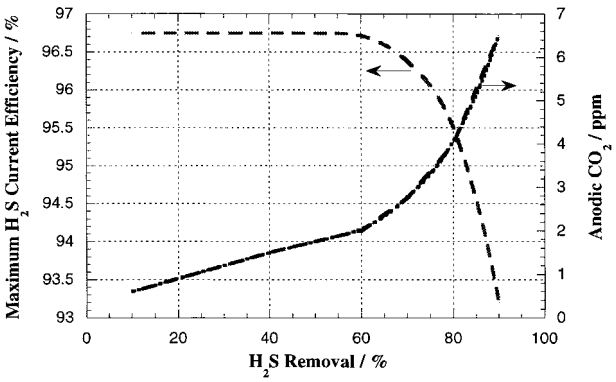


Fig. 7. Predicted anodic $CO_2$ production and maximum $H_2S$ efficiency against $H_2S$ removal. 100 ppm inlet $H_2S$.

The second is the oxidation of hydrogen and carbonate to water and carbon dioxide by

$$H_2 + CO_3^{2-} \longrightarrow H_2O + CO_2 + 2e^- \qquad (24)$$

Reaction 23 eliminates the possibility of sulfur condensation (Equation 2), but more importantly Reaction 24 is simply the reverse of Reaction 3, negating the electrochemical window shown in Fig. 2. This reaction will cause oxidation of carbonate from the anolyte, thus inducing carbon dioxide/water vapour reduction to form equivalent carbonate in the catholyte. Thus any hydrogen crossover will lead to parasitic current composed of Reaction 3 at the cathode and Reaction 24 at the anode, transporting carbonate without sulfide. As expected due to the preponderance of carbonate in the electrolyte, no $H_2S$ was detected in the anode outlet.

## 5. Comparison to past bench-scale experiments

The experimental percentage $H_2S$ removal efficiency is calculated using

$$H_2S\ \text{Removal} = \frac{(\text{Outlet } H_2S_{\text{zero current}} - \text{Outlet } H_2S_{\text{I applied}})}{(\text{Outlet } H_2S_{\text{zero current}})} \times 100 \qquad (25)$$

and the current efficiency is calculated using

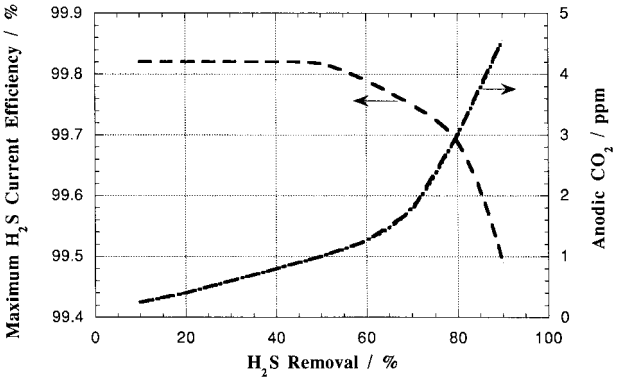


Fig. 6. Predicted anodic $CO_2$ production and maximum $H_2S$ efficiency against $H_2S$ removal. 1000 ppm inlet $H_2S$.

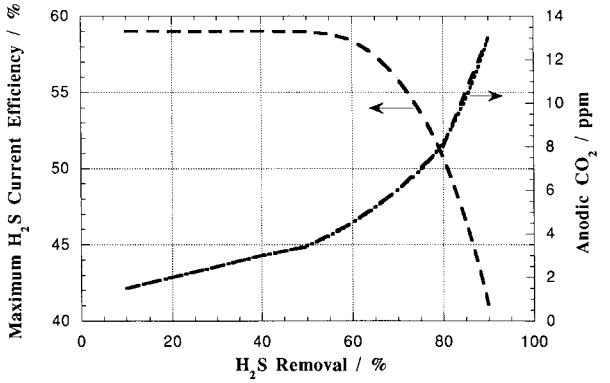


Fig. 8. Predicted anodic $CO_2$ production and maximum $H_2S$ efficiency against $H_2S$ removal. 10 ppm inlet $H_2S$.

$$\eta_{H_2S} = \frac{\%H_2S \text{ Removal (actual)}}{\%H_2S \text{ Removal (theoretical)}} \quad (26)$$

representing the ratio of $H_2S$ actually removed compared to the theoretical amount that should be removed at a finite applied current. In this Section the current efficiencies and cell potentials of bench-scale experiments previously published [13, 14], representing very sour coal gas and contaminant level coal gas, are compared to those predicted by the aforementioned theoretical prediction. Review of published results reveals that $H_2S$ current efficiencies, removal efficiencies, and cell potentials fluctuated over the duration of each experiment. This was mainly attributed to a variation in electrolyte distribution within the system, hydrogen permeation, and variable process gas seals. Actual cell potentials for polishing level experiments, graphically illustrated in this section, represent the non-IR compensated values; small applied currents coupled with low ohmic resistance resulted in an insignificant contribution, only several millivolts, to the total cell potential.

The experimental error is conservatively identified within a 95% confidence interval based on a random sampling distribution of sums and quotients, Equations 25 and 26.

### 5.1. *Contaminant level coal gas*

The polishing application of the EMS system has been demonstrated on the bench-scale level [13]. Outlet $H_2S$ levels were reduced from 10 to ~1 ppm or 90% removal. The current efficiency at this removal level was 12.6% which compared favourably to the theoretical model prediction of 30.8% current efficiency at 90% removal. $H_2S$ current and removal efficiencies are illustrated in Fig. 9. Total cell voltages at 90% removals were about −0.012 V (the theoretical value is −0.521 V). The discrepancy in actual vs predicted potentials can be explained by $H_2$ crossover, detailed earlier.

In other experiments [13], over 80% $H_2S$ removal was achieved at varying flow rates. Bench-scale current efficiencies (50% at 80% removals) agreed well with the theoretical predictions (68% at 80% removals) in a similar relationship to that of Fig. 9 (~15% below the theoretical maximum value). However, fluctuation occurred over the experimental run, due in part to a change in flow rate and electrolyte loss associated with experimental materials ($R$ varied from 1 to 3 Ω). Figure 10 gives a representative proximity of the theoretical values to bench-scale data at a cathode flow of 375 $cm^3\ min^{-1}$. Actual potentials were well below those predicted, again due to $H_2$ crossover.

### 5.2. *Very sour coal gas*

Figure 11 [14] (13000 to ~100 ppm) & Fig. 12 [13] (90 to ~6 ppm) reveal over 90% $H_2S$ removal; actual and predicted current efficiencies are shown. Once again current efficiencies are well below predicted limits. This can be attributed to hydrogen crossover due to material deficiencies. These were less evident in the polishing application of this technology due to improvements in membrane fabrication [13]. However, these results strengthened the necessity for a limiting prediction in order to gauge system performance, thereby identifying adjustments in the bench-scale apparatus necessary for improving the unit operation.

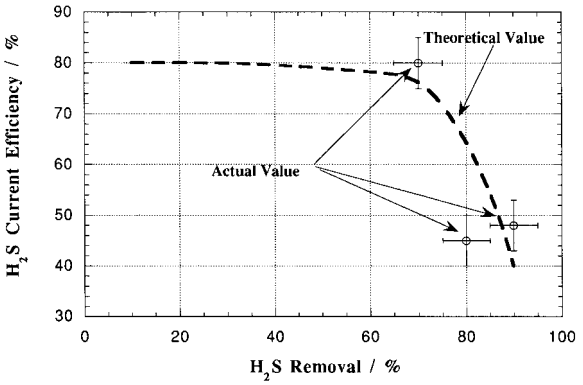


Fig. 10. Comparison of theoretical and actual values: $H_2S$ removal against current efficiency. Conditions: inlet $H_2S$ 25 ppm; temp. 650 °C; cathode flow 375 $cm^3\ min^{-1}$.

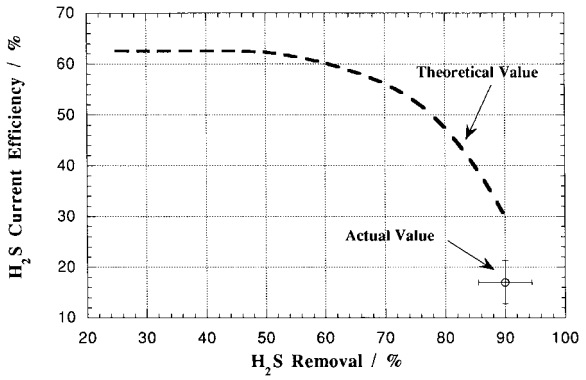


Fig. 9. Comparison of theoretical and actual values: $H_2S$ removal against current efficiency. Conditions: inlet $H_2S$ 14 ppm; temp. 650 °C; cathode flow 215 $cm^3\ min^{-1}$.

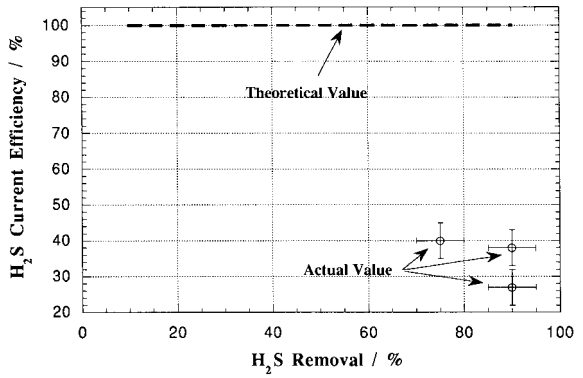


Fig. 11. $H_2S$ removal and current efficiency collected by Weaver [5] compared to theoretical model prediction. Conditions: inlet $H_2S$ 13 000 ppm; temp. 650 °C; cathode flow 75 $cm^3\ min^{-1}$.

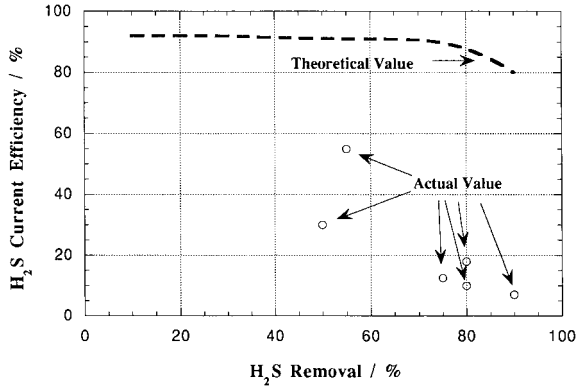


Fig. 12. $H_2S$ removal and current efficiency collected by Alexander [6] compared to theoretical model prediction. Conditions: inlet $H_2S$ 90 ppm; temp. 650 °C; cathode flow 88 $cm^3$ $min^{-1}$.

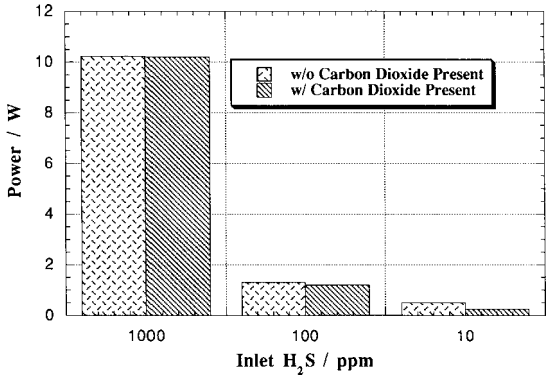


Fig. 13. Power estimates for 90% $H_2S$ removal of inlet concentration (bench-scale).

### 5.3. *Power requirements*

The results of the model reveal extremely high current efficiencies are attainable in the very sour coal gas streams (99.5% at 90% $H_2S$ removal; 1000–100 ppm). This is a favorable result considering the power requirement, given by:

$$\text{Power (P)} = \text{Total Cell Voltage (V)} \times \text{Cell Current (I)} \quad (27)$$

at higher inlet $H_2S$ concentrations is considerably greater than at lower concentrations, Fig. 13 (10.52 W at 1000 ppm inlet $H_2S$, 0.29 W at 10 ppm inlet $H_2S$); a high efficiency is a must in the higher $H_2S$ concentrations if the process is to be economically viable. Energy requirements for the 10 ppm $H_2S$ removal are negligible, shown in Fig. 13, alleviating concern due to lower current efficiencies. At any level, the *specific* theoretical energy cost at 100% current efficiency is only 0.67 kWh/kg.

## 6. Conclusions

A theoretical limiting prediction has been developed for the EMS which is used for the removal of $H_2S$ from coal gasification streams. The prediction, utilizing the salient electrochemical parameters inherent to a zero-gap membrane system, provides a performance gauge.

Comparison to experiment showed good agreement in contaminant level removal but revealed inadequacies in past bench-scale experiments with very sour coal gas. However, adjustments have recently been made based on these findings in areas of membrane manufacturing techniques and electrode stabilization. The results (in preparation for publication) are extremely positive concerning the eventual application of the EMS system on an industrial scale.

Eventual scale-up applications of this technology will utilize this theoretical limiting prediction to ensure process performance.

## Acknowledgements

The authors of this paper would like to thank the Department of Energy (DOE) and the Electric Power Research Institute (EPRI) for their continued support toward the eventual utilization of this technology for industrial scale removal of $H_2S$.

## References

[1] EPRIEM-1333, 'Assessment of Sulfur Removal Processes for Advanced Fuel Cell Systems', Final Report, C. F. Braun & Co., Alhambra, CA (Jan. 1980).
[2] E. J. Vidt, DOE/METC DE-AC-21-81MC16220, DE820-13942, Westinghouse (Dec. 1981).
[3] G. D. Focht, DOE/MC/121166-2163, DE86016041 (July 1986).
[4] S. E. Lyke, DOE/MC/19077-1803, DE8500961, Battelle Pacific Northwest Laboratories (Jan. 1985).
[5] D. Weaver, 'Electrochemical Removal of $H_2S$ from Multicomponent Gas Streams', Georgia Institute of Technology, PhD. dissertation (1988).
[6] S. R. Alexander, 'Electrochemical Removal of $H_2S$ from Fuel Gas Streams', Georgia Institute of Technology, PhD. dissertation, Atlanta, GA (1992).
[7] J. S. Robinson, 'Polishing $H_2S$ From Coal Gasification Streams Using A High Temperature Electrochemical Membrane Separation Process', Georgia Institute of Technology, PhD dissertation, Atlanta, GA (1996).
[8] E. K. Banks and J. Winnick, *J. Appl. Electrochem.* **16** (1986) 583.
[9] K. A.. White and J. Winnick, *Electrochim. Acta.* **30** (1985) 511.
[10] M. P. Kang and J. Winnick, *J. Appl. Electrochem.* **15** (1985) 431.
[11] F. P. Incropera and D. P. DeWitt, 'Fundamentals of Heat and Mass Transfer', 2nd edn, J. Wiley & Sons, New York (1985).
[12] R. S. Reid, J. M. Prausnitz and B. Poling, 'The Properties of Gases and Liquids', 4th edn, McGraw-Hill, New York (1987).
[13] D. Weaver and J. Winnick, *J. Electrochem. Soc.* **139** (1992) 492.
[14] S. R. Alexander and J. Winnick, *J. Appl. Electrochem.* **24** (1994) 1092.